A Modification of the Level Set Speed Function to Bridge Gaps in Data

Karsten Rink and Klaus Tönnies

Department of Simulation and Graphics
University of Magdeburg, Germany
{karsten, klaus}@isg.cs.uni-magdeburg.de

Abstract. Level set methods have become very popular means for image segmentation in recent years. But due to the data-driven nature of this methods it is difficult to segment objects that appear unconnected within the data. We propose a modification of the level set speed function to add a "bridging force" that allows the level set to leap over gaps in the data and segment an object despite artifacts or partial occlusions. We propose two methods to define such a force, one model-based and one image-based. Both versions have been applied to a series of test images, as well as medical data and photographic images to show their adequacy for image segmentation.

1 Introduction

Level set methods have become very popular in recent years. They have a wide range of applications in many different domains of science. Examples range from computer graphics[16], motion tracking[11], simulations of flame propagation[1] and compressible gas dynamics[9] to shortest path[3] and seismic travel time calculations[14].

Image processing is an important field for the application of level sets. Especially in image segmentation their implicit definition offers an alternative to the well-known explicit deformable models, like mass-spring-models[4] or finite element methods[8]. If the number of objects or the shape of the object that should be segmented is not known in advance, level set methods allow the definition of a model based on the properties of the desired object. This is also useful if the shape of the object has many degrees of freedom or has large variations between different data sets. Examples for their application in medical image analysis are the segmentation of the vascular tree or the bronchial tubes.

The drawback of level set methods is that artifacts distorting the data may pose a bigger problem to these methods than they do to explicit models. This is due to the data-driven nature of the front propagation process using level sets.

In this paper we propose a new force term for level set methods that allows to bridge gaps between parts of objects originating from missing information and thus to include another more model-based aspect to the definition of the speed function.

K. Franke et al. (Eds.): DAGM 2006, LNCS 4174, pp. 152–161, 2006.

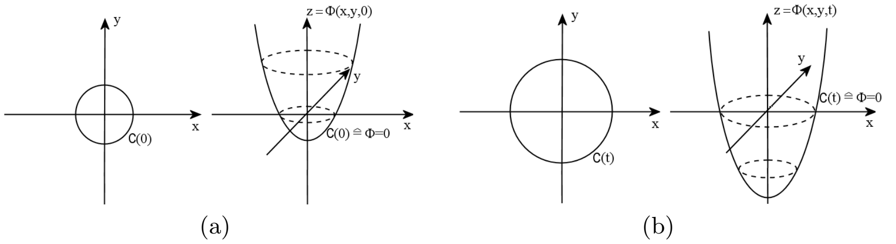

Fig. 1. Illustration of the front propagation process: The left image shows an initial curve C and the level set function Φ at time t=0. The right image shows both functions at a later time.

The paper is structured as follows: In section 2 we give a short introduction to level set methods and the definition of the speed function needed for the propagation process. Our modification of the speed function is presented in section 3. We show some experimental results in section 4 and conclude this paper in section 5.

2 Level Sets and Speed Functions

2.1 An Introduction to the Level Set Method

Level sets were introduced by Osher and Sethian [10] for the solution of surface motion problems. They are used to describe the evolution of a curve C over time according to a given speed function F.

Let $C \in \Re^n$ be a parameterised closed curve and $C(\mathbf{x})$ be the family of curves generated by the movement of the initial curve $C_{t=0}(\mathbf{x})$ along its normal direction. The speed of this movement is a function based on various elements, e.g. the local curvature of C. To allow topological changes of the evolving front, C is embedded as a zero level set into a higher dimensional function $\Phi \in \Re^{n+1}$.

$$C_{t=0}(\mathbf{x}) = \{\mathbf{x} | \Phi(\mathbf{x}, t = 0) = 0\}. \tag{1}$$

This leads to the level set equation

$$\Phi_t + F|\nabla\Phi| = 0, \tag{2}$$

where $|\nabla\Phi|$ denotes the normalised gradients of the level set function and F is the speed function determining how fast the front moves.

The advantage of this representation is that Φ always remains a function even if C splits, merges or forms sharp corners. Also, this representation is independent of the number of dimensions of C. As Φ changes over time its zero level set $\Phi(\mathbf{x}, t) = 0$ always yields the propagating front, i.e. $C(\mathbf{x})$ at time t.

An example of this process is illustrated in Figure 1.

An extensive description of the level set method with all its aspects and mathematical background can be found in [13].

2.2 Speed Functions of Level Set Applications

As mentioned in the last section, the behaviour of the front propagation process depends on the definition of the speed function F. Since the focus of this paper is the application of level set methods for image segmentation, we will discuss aspects of the speed function adequate for this application.

In contrast to explicit models used for segmentation in image processing, level sets do not have to be initialised near the the desired object boundary (although this saves computational time and usually makes the segmentation process more robust). Instead the initial contour can be placed almost anywhere, but should be located either completely inside or outside the object to be segmented.

The easiest way a speed function can be defined is simply a constant inward or outward motion F_A (also called "advection"). To assure numerical stability at shocks (e.g. corners) and to prevent the front from crossing over itself, it is necessary to use upwind schemes [10] for the calculation of the advection term. Also, the time steps Δt have to be small enough to avoid numerical instabilities[13].

The inclusion of a curvature term is also useful for many applications (e.g. it is the basis for the use of Level Sets for the simulation of compressible gas dynamics [9]), and it allows the use of front propagation methods in image analysis where noisy data and incomplete object boundaries are a common problem.

The local curvature κ is defined

$$\kappa = \nabla \frac{\nabla \Phi}{|\nabla \Phi|}. \tag{3}$$

For $C \in \Re^2$ this results in

$$\kappa = -\frac{\Phi_{xx}\Phi_y^2 - 2\Phi_x\Phi_y\Phi_{xy} + \Phi_{yy}\Phi_x^2}{(\Phi_x^2 + \Phi_y^2)^{\frac{3}{2}}}. \tag{4}$$

Depending on the characteristics of the underlying data the curvature term should be weighted to adjust its influence on the propagation process. Therefore, we will refer to the regularisation term as

$$F_\kappa = \varepsilon\kappa, \tag{5}$$

with $\varepsilon \geq 0$. Modifications of the curvature term for the calculation of Min/Max-flow are described in [6] where Level Sets are used for image enhancement.

Both, F_A and F_κ are what in explicit models (e.g. [5]) would be called "internal forces", that is, influences on the evolution of the curve that are purely model-based. A second group of forces is based on the data, therefore called "external forces". We will give here some examples that are specific to image processing applications as they incorporate image features for the modification of the speed function. The calculation of these terms will be given for 2D data sets. However, their generalisation to higher dimensions is straightforward.

Malladi et. al.[7] proposed a speed term to stop the propagating front at image gradients. One way to define such a term is

$$F_{\nabla I}^{(1)}(x,y) = \frac{1}{1 + |\nabla G_\sigma * I(x,y)|}, \tag{6}$$

where (x,y) is a pixel of the given image and $G_\sigma * I(x, y)$ denotes an image convolved with a Gaussian low pass filter with a standard deviation of σ. The new term is then incorporated into the speed function as a scalar. Therefore,

$$F = F_{\nabla I}(F_A + F_\kappa). \tag{7}$$

Another way to define this gradient-based speed term is

$$F^{(2)}_{\nabla I}(x, y) = e^{-|\nabla G_\sigma * I(x,y)|}. \tag{8}$$

This term results in smaller values near gradients and higher values in homogenous regions than given by $F^{(1)}_{\nabla I}$.

A modification of this gradient-based term was proposed by Caselles et. al.[2], who changed the speed function to

$$F = F_{\nabla I}(F_A + F_\kappa) + \nabla g \cdot \nabla \Phi, \tag{9}$$

with $g(x, y) = -|\nabla(G_\sigma * I(x, y))|$. The added term attracts the front towards edges even if it has already crossed over them. Obviously this makes the segmentation process more robust.

Other image features may be implemented in a similar fashion. For instance, an image-based speed term for a front that should just expand within a given grey value G_{seed} would be defined

$$F_G = \begin{cases} 1, & \text{if } I(x, y) = G_{seed}, \\ 0, & \text{otherwise.} \end{cases} \tag{10}$$

All image-based terms need to be combined and weighted in a meaningful fashion and may then be used the same way $F_{\nabla I}$ was used in equation (7).

There is a third group of speed terms in literature that is neither purely model-based nor data-based. We will refer to those modifications of the speed function as “geometric terms”. The given examples work in 3D, their definition in higher dimensions is more complicated than with the speed terms given above.

Van Bemmel et. al[15] define a “vesselness filter” for the segmentation of blood vessels. This function is based on the eigenvalues of the Hessian matrix at each pixel in the data set. The resulting speed term gives high values inside of cylindrical objects and low values otherwise.

A similar approach by Young et. al[8] uses a cylinder that is fitted into a volume at different angles. Here, too, grey values are used to calculate the fitting accuracy. This modification was also used for the segmentation of the vascular tree.

It is obvious that forces purely based on image features are often easy to define but have their limits with noisy data. More model-based aspects (like the mentioned “vesselness filter”) would benefit the segmentation process greatly but are usually limited to special applications. Also, the independence of the number of dimensions of the data the level set is used in is lost.

Therefore, we try to define a speed term that is somewhat weaker in its contribution to the speed function but consistent with the definition of level sets and not limited to a single application.

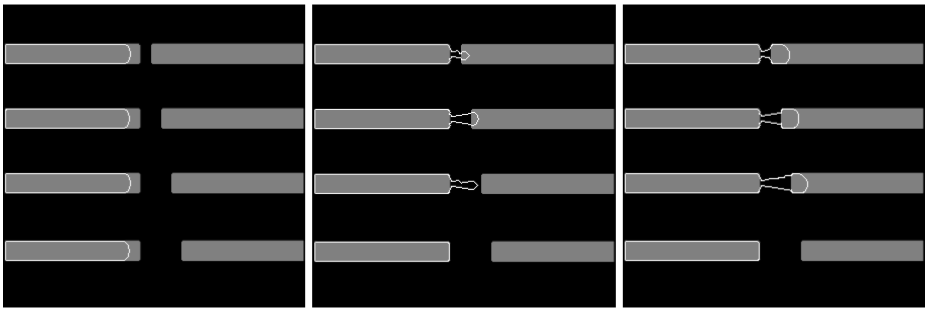

(a) (b) (c)

Fig. 2. The propagating front evolving under the new force term at three points in time. This "bridging force" is not used until the left sides of the bars are segmented. Then it lets the front leap to the right side of the bars where it continues to propagate normally. Note, that the front does not cross the gap in the bottom bar because the distance between both halves is too great.

3 Bridging Gaps in Data

The goal of this section is to define a speed term that allows the segmentation of objects whose representation in the data is disconnected. In medical imaging gaps in objects may occur due to partial volume effects when thin objects are seemingly disconnected due to a large pixel spacing in the data set. Other examples may be disconnected lines in drawings or, more generally, objects divided due to occlusions by other objects.

To solve this problem we define a new speed term that allows the propagating front to "look ahead". That is, we need to incorporate a term that for each pixel on the front decides if it should be moved even if the underlying image features in the data (grey values, gradients, etc.) suggest that it should be stopped.

The implementation is very straightforward: we calculate the surface normal for each pixel on the front. This is trivial due to the definition of level sets and is computationally inexpensive. Knowing the direction of the normal we can choose distances at which to analyse if the underlying data favours further propagation of the level set at these locations. If the data indicates that the object continues in direction of the normal, an additional force F_B is added to the speed function F, changing it to

$$F = F_I(F_A + F_\kappa) + F_B(r, i). \tag{11}$$

Here, F_I denotes the combination of all image-based speed terms as described in the previous section. The two parameters r and i of the newly defined term F_B denote the interval of the surface normal of a pixel that is examined and the sampling of the pixels in that given interval, respectively. The second parameter is only introduced to save computational cost since it is usually not necessary to analyse every pixel along the normal. Figure 2 illustrates this process. For convenience we will refer the the new speed term as “bridging force” in the remainder of this paper.

To avoid that the front leaks into the background at locations where a gap is bridged the other speed terms can be switched off. This would still connect both parts of the object but forms only very thin bridges as only very few pixels will propagate over a given gap. A better solution is an adequate definition of the other speed terms and to use e.g. curvature to avoid leaking. This strategy was used with the experiments in section 4.

This definition of the bridging force is partly image-based, as it uses image features, as well as model-based features. It assumes that regions within a certain range having the same properties belong to the same object.

Depending on the properties of the underlying data it may be difficult to define image features characteristic for a single object. The most simple feature, the grey value, may occur also in regions not belonging to the desired object.

A slight change in definition makes the bridging force purely model-based and more reliable: If the user is required to choose seed points in both parts of the disconnected object, the front approaches a gap in the representation from both sides. In this case the process of deciding if a gap should be bridged becomes much simpler because the algorithm can assert if a region is already segmented, that is, if the level set function Φ has negative values on the examined locations.

Leaking does not pose a problem if curvature is used to keep the front smooth.

Finally, note that both definitions of the “bridging force” are independent of the dimensionality of the data just as the level set method itself and may thus be used for various applications without changing their calculation.

4 Experimental Results

We now want to present some segmentation results using the new speed term.

A series of test images was prepared to determine the abilities of the segmentation using the modified speed function.

We used two classes of test images containing a total number of 180 gaps with a size between 5 and 30 pixels: class 1 are grey value images with foreground objects in various intensities, class 2 are images with white objects on a black background. Both classes of images were tested with objects of different thickness. The original images were used as well as images with added gaussian noise in various magnitudes.

Both versions of the newly defined bridge force were applied to the 180 samples. The speed function of the level set also contained the gradient- and grey value based term as well as the curvature term defined in section 2. The parametrisation of the level set was kept constant for both versions of the new speed term. Segmentation results could be more exact with an adjusted parameter set for each image but results were also satisfactory with the global set (see table 1 for an overview of the results).

Table 1. Results from the application of the modified speed function to the test images. The numbers show how many of the existing gaps in the data were crossed successfully. "Image-based" denotes the image-based version of the bridging force, "Model-based" the model-based version. Class 1 are grey value images and Class 2 are black & white images. "Class 1 > 10" and "Class 2 > 10" denote the results, if the test images containing thin structures of less than 10 pixels are left out.

Data set	All images	Class 1	Class 1 > 10	Class 2	Class 2 > 10
Overall	92%	92.5%	97.5%	91%	100%
Image-based	87%	89%	95%	83.5%	100%
Model-based	97%	96.5%	100%	98.5%	100%

Overall, 92% of the gaps within the test images were bridged correctly. We experienced problems with thin structures of less than 10 pixels width. Due to curvature it is possible that at no front pixel the gradient is directed at the target object. This effect is getting more and more unlikely the thicker the object is at the gap. Leaving out structures with 10 or less pixels thickness, only four gaps were not bridged. Examples of test images are shown in figure 3.

In images with more than 30 % added noise the front sometimes leaked out at objects and gaps if the difference between grey values of object and background was too small (see figure 3(c), for instance). Higher weights for the image-based speed terms or the curvature may prevent this, but they also prevent the bridging force from crossing over gaps in the data and extremely slow down the whole propagation process.

We also applied a level set with the modified speed function to CT data for the segmentation of blood vessels. In [12] we already used level sets for the segmentation of the vascular tree in these data sets and experienced problems with unconnected parts of vessels due to partial volume effects. First tests with the new bridging force seem promising as the modified speed function allowed the level set to connect such vessels, as depicted in figure 5.

5 Conclusions

We presented two ways to define a new speed term for a level set speed function. An image-based speed term that allows the propagating front to bridge over gaps in the presentation of an object in the data and a model-based speed term to explicitly connect fronts within a certain range of each other.

Both versions of the modified speed function were successfully applied to various test images, as well as medical data and photographic images. The system proved to be robust to noise, with the model-based speed term connecting 100% of the gaps in test images containing objects of more than 10 pixels width.

Nevertheless there are various improvements to be made. Obviously, the problem of connecting thin structures has to be solved in the future. It may help to analyse a cone in front of each pixel, instead of just the normal direction. This

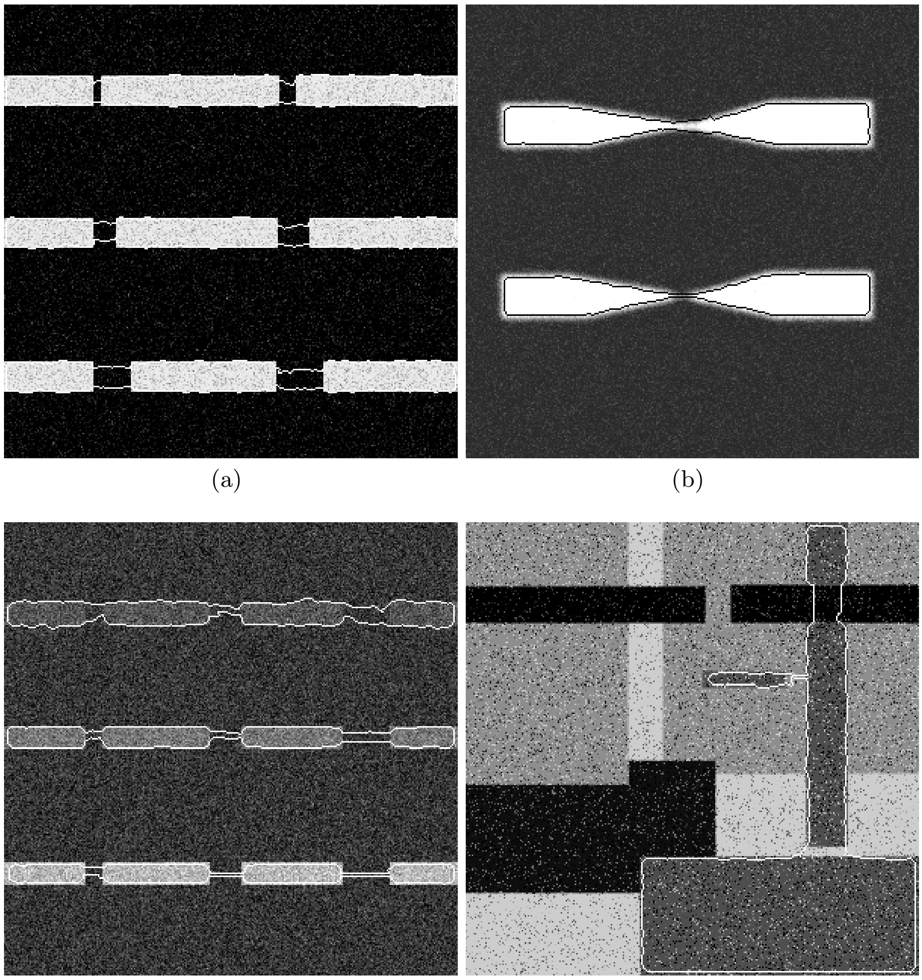

(a) (b) (c) (d)

Fig. 3. Examples of segmentation results on test images. Images (a) and (b) are of class 1, images (c) and (d) are of class 2. To all images 33% gaussian noise was added.

will slow down the propagation process significantly, though, as it will become more difficult to analyse the data ahead of the front.

Another problem are u-shaped structures that should not attract themselves via a bridging force. For the model-based speed term this could be solved with minimal computational cost by assigning an identifier to each front. In this case, the new speed term would not be applied if fronts have the same identifier. The problem is more difficult with the image-based speed term and we will hopefully solve this problem in the future.

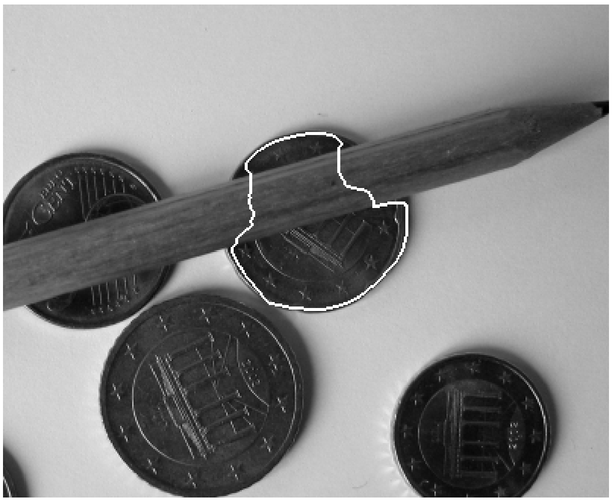

Fig. 4. Segmentation of a partially occluded object using the modified speed function. Note, that the "bridge" between both parts of the coin does neither try to approximate the occluded part of the coin nor leaks out into the occluding object. With the use of a minimum curvature speed term, as described in [6], even the occluded parts of the object should be approximated correctly.

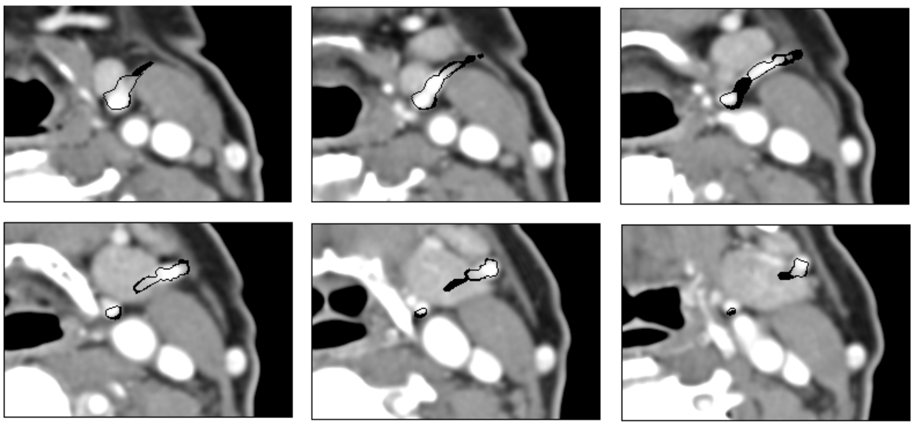

Fig. 5. Application of the modified speed function to medical images for the segmentation of blood vessels. The images show six successive slices of a CT data set with a slice spacing of 3 mm. A vessel branches off at a steep angle and due to partial volume effects the lower and upper part of the vessel seem disconnected. This makes it impossible for a level set without the additional bridging force to connect both parts of the vessel. Using our additional speed term, the level set segments the vessel correctly.

References

1. Abu-Gharbieh, R., Gustavsson, T., Kaminski, C., Hamarneh, G.: Flame Front Matching and Tracking in PLIF Images using Geodesic Paths and Level Sets. IEEE Int. Conf. on Comp. Vis., Workshop on Variational and Level Set Methods in Comp. Vis. (2001) 112–118.
2. Caselles, V., Kimmel, R., Sapiro, G.: Geodesic Active Contours. Int. J. Comp. Vis. **22**(1) (1991) 61–79
3. Deschamps, T.: Curve and Shape Extraction with Minimal Path and Level-Set techniques. Applications to 3D Medical Imaging. Ph.D. thesis. L'Univerité de Paris-Dauphine. (2001)
4. Hamarneh, G., McInerney, T., Terzopoulos, D.: Deformable Organisms for Automatic Medical Image Analysis. MICCAI 2001. 66–76
5. Kass, M., Witkin, A., Terzopoulos, D.: Snakes: Active Contour Models. Int. J. Comp. Vis. **1**(4) (1988) 321–331
6. Malladi, R., Sethian, J. A.: Image Processing: Flows under Min/Max Curvature and Mean Curvature. Graph. Mod. and Image Proc. **58**(2) (1996) 127–141
7. Malladi, R., Sethian, J. A., Vemuri, B.: Shape Modelling with Front Propagation: A Level Set Approach. IEEE Trans. on PAMI. **17**(2) (1995) 158–175
8. McInerney, T., Terzopoulos, D.: A Dynamic Finite Element Surface Model for Segmentation and Tracking in Multidimensional Medical Images with Application to Cardiac 4D Image Analysis. Comput. Med. Imaging Graph., **19**(1) (1995) 69–83
9. Mulder, W., Osher, S. J., Sethian, J. A.: Computing Interface Motion in Compressible Gas Dynamics. J. Comp. Phys. **100** (1992) 209–228
10. Osher S., Sethian, J. A.: Fronts Propagating with Curvature Dependent Speed: Algorithms Based on Hamilton-Jacobi Formulation. J. Comp. Phys. **79** (1988) 12–49
11. Paragios, N., Deriche, R.: Geodesic Active Contours and Level Sets for the Detection and Tracking of Moving Objects. IEEE Trans. on PAMI. **22**(3) (2000) 266–280
12. Rink, K., Törsel, A. M., Tönnies, K.: Segmentation of the Vascular Tree in CT Data using Implicit Active Contours. Bildverarbeitung für die Medizin 2006. 136–140
13. Sethian, J. A.: Level Set Methods and Fast Marching Methods. Cambridge University Press. (1999)
14. Sethian, J. A., Popovici, A. M.: 3-D traveltime computation using the fast marching method. Geophysics. **64**(2) (1999) 516–523
15. Van Bemmel, C. M., et. al.: A Level-Set-Based Artery-Vein Separation in Blood-Pool Agent CR-MR Angiograms. IEEE Trans. Med. Imag. **22**(10) (2003) 1224–1234
16. Whitaker, R. T.: Isosurfaces and Level-Set Surface Models. Technical Report UUCS-02-010. School of Computing, Univ of Utah. (2002)
17. Young, S., Pekar, V., Weese, J.: Vessel Segmentation for Visualization of MRA with Blood Pool Contrast Agent. MICCAI 2001. 491–498